

Entanglements of Semidilute Polymer Rods

Marshall Fixman

Department of Chemistry, Colorado State University, Fort Collins, Colorado 80523

(Received 25 October 1984)

Brownian simulations of semidilute rods confirm that rotation of rods is ordinarily confined to cages which break up through diffusion along rod axes. However, the angular width of the cages is proportional to $1/(cL^3)^p$ if the rods are thin, with $p = \frac{1}{2}$ rather than the previously supposed $p = 1$. The latter result is found only for rods at true equilibrium, which cannot occur unless cage topology equilibrates as fast as cage size.

PACS numbers: 61.25.Hq, 05.60.+w, 36.20.Ey

As the simplest examples of entangling polymers,¹⁻³ semidilute solutions of long rods have considerable interest. The Doi-Edwards^{1,2} theory (DET) predicts definite scaling relations between the rotational diffusion constant D_{rot} and the concentration c and length L of the rods. The conventional faith that scaling coefficients are near unity then leads to D_{rot} values that are much smaller than observed values in the accessible range of the dimensionless parameter cL^3 . This work reports on Brownian simulations of the rotational time correlation function $C(t)$. The results lead to the conclusion that a DET is correct in its picture of rotational diffusion as motion within cages that are occasionally dissolved by diffusion along rod axes. However, the results and mean-field arguments show that DET is incorrect in its calculation of cage sizes, because of an unwarranted assumption that the rods are at equilibrium. This conclusion is not based on cage sizes or D_{rot} alone; DET actually gives larger cage sizes throughout most of the studied range of cL^3 than the proper ensemble, but predicts much too rapid a decrease of cage size with increasing cL^3 and cannot fit the $C(t)$ data. A revised theory is in good agreement with the simulations. The following points will be considered: the physical model and methods used for the simulation, the formalism used to describe and analyze the results, the results themselves, and a mean-field rationalization.

For the simulations each rod was constructed as a chain of three beads. The two bonds within a rod were constrained by vibrational forces to prescribed fluctuations of length and relative angle. The work reported here concerns only quite rigid, straight rods. A program designed for the general study of internal motion in polymer chains was used with slight modification: (1) The vibrational force constants that restrict the relative motion of successive beads were set to 0 after every third bead. (2) Hydrodynamic interaction between beads was suppressed. (3) The interaction potential between beads was replaced by an interaction between bonds, namely, $(\epsilon/\sin\omega)\sigma^{-1}\exp(-\sigma r_0^2)$, where r_0 is the shortest distance between two bonds, ω is the crossing angle between them, and ϵ and σ are parameters discussed below. The units of energy, dis-

tance, and time were $k_B T$, b , and $\beta b^2/k_B T$, respectively, where b is a reference unit of length and β is the friction constant of the end beads. The chosen parameter values, usually $\epsilon = 100$ and $\sigma = 12$, give a potential strong enough that rod crossings were never observed in studies designed to show them. They might have occurred on occasion, but the results on rotational motion in frozen environments show that crossings were statistically insignificant.

A more elaborate formalism than that of DET is used for analysis of the simulations, in order to bridge the gap between short-time caged motion and long-time exponential decay. The formalism describes the angular motion of a rod in terms of the position of an end bead on the spherical surface of radius $L/2$; see Doi.¹ The two-component bead velocity vector \mathbf{v} on the surface is assumed to obey the equation

$$m_e d\mathbf{v}/dt = -\beta_e \mathbf{v} - \int_0^\infty K(\tau) \mathbf{v}(t-\tau) d\tau + \mathbf{F}(t), \quad (1)$$

where $\mathbf{F}(t)$ is a random force with a spectral density inferred from the memory function $K(t)$ by standard means.⁴ The effective friction constant $\beta_e = 2\beta = 2$ in the chosen units, and the mass m_e is set equal to zero. The combination of memory and a moving frame might present severe difficulty but for the fact that the memory is short on the time scale of frame rotation. Sequences of random displacements, with the proper covariance computed from Eq. (1), were generated on a tangent plane and mapped onto the spherical surface. The calculated $C^c(t) = \langle \cos\theta(t) \rangle$, where $\theta(t)$ is the rotational displacement in time t , is an average over such sequences, and is compared with the simulation results.

Simulations were carried out for three levels of motional freedom, in order to study, first, rotational motion in frozen environments; second, rotational equilibration of cage sizes; and third, completely free motion. The levels are defined as follows. (1) One rod is allowed to rotate in the rigid cage provided by its neighbors. Translational motion is eliminated by the assignment of a very large friction constant to the middle bead. (2) All rods in the system are allowed to ro-

tate but not translate. (3) All rods are allowed to rotate and translate, and all beads have $\beta = 1$. All systems were initiated with a uniform distribution of rod orientation and centers and were well aged before sampling, except for a few special studies discussed below.

The first question to be addressed is the extent of rotational freedom with level-1 freezing. Individual rods in systems with small cL^3 on occasion showed more than one plateau in $C(t)$, as the rod diffused out of a partial cage, but the average $C(t)$ always showed steady decay to a single plateau $C_p = C(\infty)$. Equation (1) with $K(t) = K_0$, an elastic restoring force constant, was therefore used to describe level-1 motion. Observed values of C_p for various rod number densities c and rod lengths L are given in Table I. C_p^{f} and C_p^{d} values apply to unaged systems and will be discussed below.

The calculated values C_p^{f} and ρ in Table I were obtained as follows. The mean square displacement of an elastically constrained bead on the spherical surface is $\rho^2 \equiv \langle r^2 \rangle = 2/K_0$. Since ρ is small, $C_p^{\text{f}} \approx 1 - \langle \theta^2 \rangle / 2 = 1 - 4\rho^2 / L^2$. (A factor of 2 enters because the value of $\langle \theta^2 \rangle$ in C_p^{f} measures relative displacements along a trajectory, and ρ^2 measures displacements from the equilibrium point established at $t = -\infty$.) ρ is assumed to be related to its value ρ_0 for infinitely thin rods by $\rho = \rho_0 - d$, following Doi,¹ and ρ_0 is assumed to be given by

$$\rho_0^2 = \alpha / cL, \quad (2)$$

where α and d are parameters. To fit the observed ρ 's, it is necessary to use Eq. (2) rather than DET, which has an additional divisor of cL^3 on the right-hand side. The values used for the two parameters were $\alpha = 0.7$ and $d = 1.2$. The latter value is much larger than might have been predicted from the bond pair interaction potential. However, d actually refers to the projected motion on the spherical surface; the projection stretches the effective range of interaction and makes d a complicated average over the statistical properties

of the rod distribution. A single check of the relation between d and the potential parameters ϵ and σ was made; d seems to change in rough rather than exact proportion to the potential width.

Level-2 systems showed extensive and rapid orientational equilibration of the rods making up a cage, but an extremely slow drift of the center of the cage. Because of that it seemed reasonable to neglect this drift entirely in a first interpretation of unrestricted motion, level 3, and to ascribe all the relaxation of $K(t)$ to the onset of translational motion.

In level-3 motion, all three beads on a rod are assigned the same friction constant, unity, and the calculated results are compared with simulations on the basis of $K(t) = K_0 \exp(-Rt)$, where K_0 is calculated as described above. Both the simple decay law and the transferability of K_0 values from levels 1 to 3 are tested by the comparison. According to DET, the relaxation process is induced solely by translational diffusion parallel to the rod axis, and consequently

$$R = \gamma D_{\parallel} / L^2, \quad (3)$$

where D_{\parallel} is the diffusion constant and γ is a constant. In the present work $D_{\parallel} = k_B T / 3\beta$ in physical units, or $\frac{1}{3}$ in the reduced units. The comparison between theoretical and simulation results shown in Fig. 1 is based on $\gamma D_{\parallel} = 90$, and on the values $\alpha = 0.7$ and $d = 1.2$ previously inferred from level-1 results. Deviations are comparable to the statistical error of the simulations.

Given the good agreement between the simulations and the revised calculation, it remains to rationalize Eq. (2) and to discover the defect in DET. As before, the orientation of a probe rod is characterized by the position of one of its end beads on the spherical surface of radius $L/2$. The end bead is considered to be caged within a circle of radius ρ_0 , corresponding to an angular rotation $\theta \equiv 2\rho_0 / L$. Some cL^3 other rods have projections on the surface and might contribute to caging the probe rod. These projections are themselves

TABLE I. Simulation and theoretical plateau values $C(\infty)$ for various parameter sets. C_p^{f} and C_p^{d} plateau values apply to systems selected from the initially random distribution. C_p and ρ values apply to dynamically aged systems. C_p^{e} is calculated for true equilibrium; C_p^{f} and ρ are calculated for constrained (dynamic) equilibrium. N is the number of rods in the basic simulation cell. Standard deviations of simulation results are shown in parentheses in units of the last digit.

System	cL^3	L	N	C_p	C_p^{f}	ρ	C_p^{e}	C_p^{d}	C_p^{e}
1	48.53	60	100	0.956(8)	0.9599	6.01	0.83(3)	0.87(4)	0.8435
2	97.06	50	100	0.987(2)	0.9852	3.05	0.962(6)	0.968(10)	0.9679
3	113.37	46	150	0.989(2)	0.9890	2.41	0.9787
4	145.59	50	150	0.992(1)	0.9918	2.27	0.988(2)	. . .	0.9882
5	218.38	50	225	0.996(1)	0.9957	1.63	0.996(1)	0.996(1)	0.9962

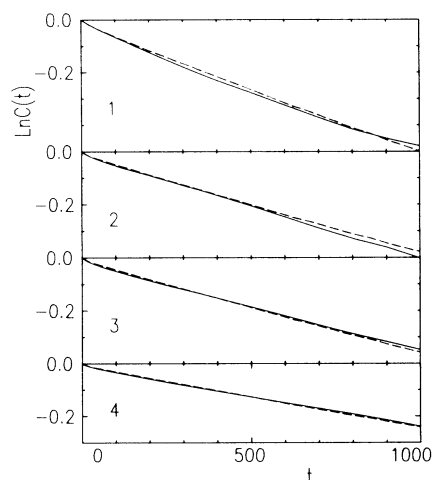


FIG. 1. Rotational time correlation functions vs t for systems 1 through 4 of Table I. Solid curves are simulation results and dashed curves are calculated from the relaxation model of Eq. (1).

allowed to rotate only within the projections of cages, namely sectors, of mean angular size θ_m . As θ increases from an infinitesimal reference value θ_r , the change in entropy of the system will be

$$\Delta S = k_B \ln(\theta/\theta_r)^2 - N_m l_m \theta, \quad (4)$$

where $l_m \theta$ is the decrease in cage size available to any of N_m projections on the surface and l_m is a constant. Maximization of ΔS with respect to θ occurs at $\theta_m = k_m/N_m$, where k_m is another constant. DET results from the supposition that $N_m = cL^3$. However, only those rods lying within a sector that includes the probe are able to recognize and equilibrate with the probe, unless they diffuse by translational motion out of their cages and into the proper sector. But such motion contradicts the supposition of definite cages, which equilibrate with respect to size but not topology during extended intervals between cage breakup. As the chance that a projection lies within any sector is proportional to θ_m , N_m is proportional to $cL^3 \theta_m$, and this gives Eq. (2) rather than DET.

The preceding considerations indicate that transla-

tional averaging must be suppressed in the calculation of cage sizes. The failure of an equilibrium ensemble to give correct cage sizes is illustrated by the simulation results C_β^x and C_β^y in Table I. C_β^x applies to a single rod and averages over environments; C_β^y averages over different rods for a single configuration. For either sampling, configurations were chosen from a uniform distribution of centers and orientations, and were unaged. This ensemble should be close to the true equilibrium ensemble of thin but finite rods. The equilibrium cage sizes are quite different from the dynamical values, but agree quite well with the values C_β^{xc} calculated from DET with $\rho_0^2 = 105/c^2 L^4$, $\rho = \rho_0 - d$, and $d = 0.8$.

It seems necessary to conclude that the Brownian model, and probably a real system as well, reaches only a constrained rather than a true equilibrium distribution of cage sizes, and in a sense is nonergodic. Molecular dynamics simulations,⁵ without solvent friction, do confirm DET scaling at high densities, but because $D_{||} \rightarrow \infty$ under the same conditions,⁵ there seems to be no conflict. The observed failure of ergodicity rests on the rapid equilibration of cage sizes, and the slow breakup of cage topology. Mathematical rods⁵ in the absence of solvent friction do not satisfy this condition. The nature of the quasithermodynamic transition from complete to partial equilibrium is an interesting subject for speculation. For sufficiently large cL^3 and small $D_{||}$, the system seems to purchase rotational entropy at the expense of translational.

This work was supported in part by National Institutes of Health Grant No. NIH GM 27945.

-
- ¹M. Doi, J. Phys. (Paris) **36**, 607 (1975).
²M. Doi and S. F. Edwards, J. Chem. Soc. Faraday Trans. **2** **74**, 560 (1978).
³M. Doi and S. F. Edwards, J. Chem. Soc. Faraday Trans. **2** **74**, 1789 (1978).
⁴L. D. Landau and E. M. Lifshitz, *Statistical Physics* (Addison-Wesley, Reading, Mass., 1969), Chap. 12.
⁵D. Frenkel and J. F. Maguire, Mol. Phys. **49**, 503 (1983).